JARO 20: 233–245 (2019)
DOI: 10.1007/s10162-019-00719-1

JARO
Journal of the Association for Research in Otolaryngology

Research Article

Early Hearing Loss upon Disruption of Slc4a10 in C57BL/6 Mice

Antje K. Huebner,[1] Hannes Maier,[2] Alena Maul,[3] Sandor Nietzsche,[4] Tanja Herrmann,[1] Jeppe Praetorius,[5] and Christian A. Hübner[1]

[1]*Institute of Human Genetics, Jena University Hospital, Friedrich Schiller Universität, Am Klinikum 1, 07747, Jena, Germany*

[2]*Department of Otolaryngology and Cluster of Excellence Hearing4all, Deutsches HörZentrum Hannover, Medical University Hannover, Karl-Wiechert-Allee 3, 30625, Hannover, Germany*

[3]*Max-Delbrück Centrum für Molekulare Medizin (MDC) and NeuroCure, Robert-Rössle-Str. 10, 13092, Berlin, Germany*

[4]*Electron Microscopy Center, Jena University Hospital, Friedrich Schiller Universität, Ziegelmühlenweg 1, 07743, Jena, Germany*

[5]*Department of Biomedicine, Health, Aarhus University, Aarhus, Denmark*

Received: 7 February 2017; Accepted: 25 March 2019; Online publication: 18 April 2019

ABSTRACT

The unique composition of the endolymph with a high extracellular K^+ concentration is essential for sensory transduction in the inner ear. It is secreted by a specialized epithelium, the stria vascularis, that is connected to the fibrocyte meshwork of the spiral ligament in the lateral wall of the cochlea via gap junctions. In this study, we show that in mice the expression of the bicarbonate transporter Slc4a10/Ncbe/Nbcn2 in spiral ligament fibrocytes starts shortly before hearing onset. Its disruption in a C57BL/6 background results in early onset progressive hearing loss. This hearing loss is characterized by a reduced endocochlear potential from hearing onset onward and progressive degeneration of outer hair cells. Notably, the expression of a related bicarbonate transporter, i.e., Slc4a7/Nbcn1, is also lost in spiral ligament fibrocytes of Slc4a10 knockout mice. The histological analysis of the spiral ligament of Slc4a10 knockout mice does not reveal overt fibrocyte loss as reported for Slc4a7 knockout mice. The ultrastructural analysis, however, shows mitochondrial alterations in fibrocytes of Slc4a10 knockout mice. Our data suggest that Slc4a10 and Slc4a7 are functionally related and essential for inner ear homeostasis.

Correspondence to: Christian A. Hübner · Institute of Human Genetics · Jena University Hospital, Friedrich Schiller Universität · Am Klinikum 1, 07747, Jena, Germany. email: Christian.huebner@med.uni-jena.de

Keywords: bicarbonate transport, Slc4a10, Slc4a7, NCBE, deafness, fibrocyte, pH

INTRODUCTION

The steep K^+ gradient and the positive endocochlear potential (EP) between the endolymph, which bathes the apical poles of hair cells and the perilymph at their basolateral site, result in a depolarizing K^+ influx upon sound-induced opening of mechanosensitive cation channels in hair cell stereocilia. The K^+ gradient and the EP are generated by the stria vascularis in the lateral wall of the cochlea that secretes K^+ into the endolymph. Basal cells of the stria vascularis are coupled with fibrocytes of the spiral ligament (SL) via gap junctions.

A second gap junction system connects supporting cells of the organ of Corti surrounding the basal poles of hair cells and the root cells whose processes penetrate the spiral ligament. The importance of this gap junction system for hearing is highlighted by the multitude of genes encoding gap junction proteins expressed in the inner ear, such as Connexin-26, -30, -31, and -43 (Petit et al. 2001). Hearing loss may result from defective shuttling of ions, nutrients, or second messengers in the inner ear. Notably, many of the ion transport proteins expressed along this pathway have been identified through mutations in mice and

humans that lead to deafness. This list comprises KCl co-transporters KCC3 (Boettger et al. 2003) and KCC4 (Boettger et al. 2002), the Cl^-/HCO_3^- exchanger SLC26A4/Pendrin (Everett et al. 2001), the Na^+-HCO_3^- co-transporter SLC4A7 (Bok et al. 2003), and SLC4A11 (Desir et al. 2007; Groger et al. 2010). The latter, a borate transporter, also conducts Na^+ and OH^- in the absence of borate (Park et al. 2004).

Like SLC4A7 and SLC4A11, SLC4A10 belongs to the SLC4 family of bicarbonate transporters (Romero et al. 2013). SLC4A10 utilizes the transmembrane gradient of Na^+ to drive cellular net uptake of HCO_3^- and, thus, acid extrusion. Though SLC4A10 was first reported to mediate Na^+-dependent Cl^-/HCO_3^- exchange (NCBE) (Wang et al. 2000), human SLC4A10 might not require Cl^-, which is consistent with electroneutral Na^+/HCO_3^- cotransport (Parker et al. 2008). In hippocampal neurons of Slc4a10 knockout mice, acid extrusion was impaired (Jacobs et al. 2008). These mice display an increased seizure threshold (Jacobs et al. 2008; Sinning et al. 2015) and impaired vision (Hilgen et al. 2012). In agreement with a role in the production of cerebrospinal fluid, brain ventricles of Slc4a10 knockout mice were collapsed (Jacobs et al. 2008). More recently, a study identified Slc4a10 as a novel late-onset hearing loss gene in a screen for age-related phenotypes in mice in a mixed C3H.Pde6b+ background (Potter et al. 2016).

In this study, we show that Slc4a10 disruption in a C57BL/6J background results in early-onset severe hearing loss with a reduced endocochlear potential (EP). We further show that disruption of Slc4a10 results in loss of Slc4a7 expression specifically in inner ear fibrocytes but not in other tissues. At the ultrastructural level, mitochondria of spiral ligament knockout fibrocytes show severe alterations. Thus, our data link Slc4a10 and Slc4a7 functions in the inner ear and highlight the importance of the genetic background for the analysis of inner ear phenotypes in mice.

MATERIALS AND METHODS

Animals

All experiments were approved by the responsible local institution (Landesamt für Lebensmittelsicherheit und Verbraucherschutz, Bad Langensalza and Niedersächsisches Landesamt für Verbraucherschutz und Lebensmittelsicherheit, Germany) and comply with the ARRIVE guidelines. The generation of Slc4a10 knockout mice from a 129SvJ embryonic stem cell line was described previously (Jacobs et al. 2008). All studies were performed in mice that were backcrossed with C57BL/6J for at least 15 generations.

Mice with a targeted disruption of the *slc4a7* gene (Boedtkjer et al. 2011) were obtained from embryonic stem cells (40G1; Centre for Modeling Human Disease, Toronto, Canada) containing the pMS1 gene trap vector integrated 434 bases upstream of the start codon. Heterozygous mice were backcrossed into wild-type C57BL/6J mice for more than 15 generations before use. Breeding and use of the mice were approved by the Danish Animal Experiments Inspectorate.

In Vivo Recordings of Auditory Brainstem Response

Auditory-evoked brain stem responses to clicks were recorded in anesthetized animals (16 mg/kg xylazine hydrochloride, 60 mg/kg *S*-ketamine hydrochloride) on a heating pad in a soundproof chamber. Acoustic click stimuli were delivered monaurally using a Beyer DT-48 earphone and were monitored with a probe microphone (MK301, Microtech Gefell) integrated into the earpiece. Bioelectric potentials were recorded by subcutaneous silver electrodes at the vertex (reference), forehead (ground), and ventrolateral to the stimulated ear. Alternating clicks (200 µs duration) were applied at a rate of 21/s and averaged 400–2000 times. Stimulus intensities started at 118 dB peak equivalent SPL (pe dB SPL) in increments of 20 dB except near threshold where 5 dB steps were used. The hearing threshold was defined as the lowest intensity to generate a reproducible auditory-evoked brain stem response wave form.

Endocochlear Potential Measurements

The endocochlear potential (EP) was measured in anesthetized mice (14 mg/kg xylazine hydrochloride, 80 mg/kg ketamine hydrochloride) on a heated surgical table. The bulla was opened laterally, leaving the tympanic membrane intact. The bone over the first turn of the cochlea was thinned and opened below the stapedial artery. A single-barreled microelectrode was inserted. Voltage was measured against a reference electrode below the skin on the neck of the animal.

Histology and Immunohistochemistry

Inner ears were removed, post-fixed in 4 % paraformaldehyde in phosphate buffered saline (1x PBS) and, if necessary, decalcified in 10 % EDTA in PBS over night at 37 °C. HE-histology of 8-µm cochlea cross-sections was performed following standard protocols. For immunohistochemistry, inner ears were treated as described previously (Hennings et al. 2012). The polyclonal antibody against the Slc4a10 protein was raised in rabbits and guinea pigs. The antibody

was affinity purified as described previously (Jacobs et al. 2008). The antiserum against Pendrin was provided by C.A. Wagner. The mouse anti rat Cx 26 (Gjb2), rabbit anti mouse Cx 30 (Gjb6) antibodies (Zymed 13–8100 and 71–2200), the rabbit anti mouse Slc4a7 antibody (LSBio, LS-B13709), and the monoclonal anti mouse cytochrome C antibody (abcam, ab3256, clone 6H2.84) were used following the instructions of the respective provider. Undecalcified tissue was used for immunostainings with the anti Slc4a7 antibody. Immunostainings were performed on 5-µm cryo-sections of at least 2 independent mice per genotype and were analyzed with a confocal microscope (Zeiss LSM 510 or 880, Germany).

For phalloidin staining, basilar membranes of fixed inner ears were removed and stained with Alexa-555-conjugated phalloidin in 1 × PBS/TX-100 for 20 min. For quantification of outer hair cell loss, outer hair cells were counted for the basal, middle, and apical basilar membrane corresponding to 30 Deiters' cells from 3 to 5 mice per genotype and age. Each mean value was calculated from 3 to 13 sections.

For western blot analysis, spiral ligaments of 3 mice per genotype and age (3, 6, and 56 weeks of age) were pooled and homogenized in lysis buffer (30 mM Tris-HCl, 5 mM EDTA, 3 mM NaF, 10 % Glycerol, 3 % SDS, supplemented with complete (Sigma-Aldrich, St. Louis, MO, USA)), separated by SDS-PAGE (gel 12 %) and blotted onto nitrocellulose membranes. For immunodetection, membranes were incubated over night at 4 °C with primary antibodies, diluted 1:500 in 3 % milk/TBST. After washing, the membranes were incubated for 2 h at room temperature with secondary antibodies in TBST. Beta-actin (Santa Cruz, sc-47778) served as a loading control.

The ImageJ software was used to determine the number of nuclei in the spiral ligament in 8-µm thick HE-stained paraffin sections with identical parameters and threshold adjustments for all sections.

CytC signals were quantified in type II fibrocytes (% of area) from 3 mice per genotype and 2 sections each at the age of 24 weeks. For this purpose, 5-µm thick cryo-sections of one WT and one KO cochlea were mounted on the same slide. All slides were treated in parallel. Images were taken at × 100 magnification with identical microscope settings. Rectangular regions of interest of the same size were positioned in the center of the type II fibrocyte region and analyzed with the ImageJ software using identical parameters and threshold adjustments.

Ratiometric pH Measurements

Because Slc4a10 mediates acid extrusion, we assessed whether pH regulation is compromised in fibrocytes of Slc4a10 knockout mice. For pH measurements, the cochlea capsule was dissected from mice aged between P11 and P13. Lateral wall tissue was obtained by microdissection in gluconate solution containing (mM): 104 NaCl, 3 KCl, 2 $CaCl_2$, 1.1 NaH_2PO_4, 2 $MgSO_4$, 25 $NaHCO_3$, 10 D-glucose, 20 Na-gluconate (pH 7.2, 300 mosmol, saturated with 95 % O_2, 5 % CO_2). Great care was taken to keep the stria vascularis attached to the underlying spiral ligament. Lateral wall tissue was loaded with 5 µM BCECF-AM (Molecular Probes) for 35 min at 37 °C. The tissue was mounted in a bath chamber on an upright microscope (Axio Observer.Z1, Zeiss) and superfused with gluconate solution at a speed of 2 ml/min (i.e., 2 bath changes per min). To evoke pH_i changes, Na-gluconate was exchanged by 20 mM propionate. Fluorescence was measured at 436 nm and 495 nm excitation wavelengths using the MetaFluor imaging software (Visitron). From each spiral ligament, the ratio was obtained from 3 fibrocytes at room temperature. The pH_i signals from individual fibrocytes were averaged per spiral ligament before averaging across spiral ligaments from different mice. The fluorescence ratio was converted to pH according to a calibration performed in BCECF-loaded HEK cells in HEPES buffered solution of varying pH containing (mM): 140 KCl, 50 NMDG, 30 Hepes, 10 D-glucose, 5 $MgSO_4$, 0.01 Nigericin (Sigma-Aldrich, St. Louis, MO, USA).

Ultrastructural Analysis of Spiral Ligament Fibrocytes

For transmission electron microscopy (TEM), mice were anesthetized and perfused with PBS followed by a mixture of 4 % paraformaldehyde (PFA) and 1 % glutaraldehyde in PBS (pH 7.4). Cochleae were removed, spiral ligaments dissected and fixed overnight in perfusion fixative at 4 °C. After washing with 0.1 M cacodylate buffer (pH 7.4), a post-fixation with 1 % (*w/v*) osmium tetroxide in cacodylate buffer for 1 h was performed followed by dehydration in ascending ethanol series, including staining with uranyl acetate at the 50 % step. The samples were then embedded in epoxy resin (Araldite). A total of 700-nm semi-thin sections were cut with the Ultracut E (Reichert-Jung, Germany), stained with toluidine blue, and analyzed by light microscopy (Axio, Lab.A1, Zeiss, Oberkochen, Germany). Ultrathin sections were cut with a LKB Ultratome III (LKB, Sweden). After mounting on filmed Cu grids and post-staining with lead citrate, the sections were studied in a transmission electron microscope (EM 900, Zeiss, Germany).

Statistics

If not noted otherwise, data are presented as mean +/- SEM. Normal distribution of data was tested by Shapiro-Wilk test. Statistical evaluation was performed

by either Student's *t* test of normally distributed data or Mann-Whitney rank sum test in case of non-parametrically distributed data. In experiments that included repeated measurements, differences between groups were tested by repeated-measures ANOVA. If necessary, two-way ANOVA and post-test Bonferroni analysis were applied. All statistical tests were performed with SigmaPlot 12.5 (Systat GmbH, Germany), IBM SPSS Statistics for Windows, Version 21.0 (IBM Corp, USA), or Microsoft Excel (Microsoft, USA). The respective statistical test is indicated.

RESULTS

Slc4a10 Is Expressed in Spiral Ligament Fibrocytes of the Cochlea

Because disruption of both Slc4a7 (Bok et al. 2003) and Slc4a11 (Desir et al. 2007; Groger et al. 2010) causes deafness, we decided to assess whether the closely related transporter Slc4a10 is also expressed in the inner ear. We performed stainings of cochlear sections from adult wild-type mice with an antibody directed against Slc4a10, as previously described (Jacobs et al. 2008). Following the classification of fibrocytes into different subgroups by Spicer and Schulte (Spicer and Schulte 1991), type I, II, IV, and V fibrocytes in the lateral wall of the cochlea were intensely labeled for Slc4a10 (Fig. 1a, b). This signal was specific because it was absent from stained Slc4a10 knockout cochlea sections (Fig. 1c). No overlap was observed with Pendrin (Fig. 1a, b), which localized to the apical membrane of spiral prominence epithelial cells, spindle-shaped cells, and root cells of the lateral wall as previously reported (Wangemann et al. 2004).

Next, we addressed the developmental profile of Slc4a10 expression in the inner ear of mice (Fig. 1d–i). Slc4a10 expression started between postnatal day (P) 7 and 9 in type II and V fibrocytes (Fig. 1e, f) and then spread to type I and IV fibrocytes (Fig. 1a, b, i). Notably, cells of the organ of Corti and the stria vascularis were unlabeled at all developmental stages analyzed.

Acid Extrusion Is Preserved in Fibrocytes of P12 Slc4a10 Knockout Mice

Disruption of Slc4a10 in mice impairs acid extrusion in hippocampal pyramidal neurons (Jacobs et al. 2008). We tested whether the regulation of the intracellular pH (pH_i) of inner ear fibrocytes is impaired upon disruption of Slc4a10. We dissected the spiral ligaments from WT and KO mice between P11 and P13, when Slc4a10 is already partially expressed but the bony capsule of the inner ear is not yet fully calcified. Ratiometric pH measurements with BCECF-AM (2′,7'-Bis-(2-Carboxyethyl)-5-(and-6)-Carboxyfluorescein, acetoxymethyl Ester), which allow correction for variable dye loading, dye leakage, or detector sensitivity were conducted. The measurements did not show any difference in either the maximal peak acidosis in response to propionate or the alkaline overshoot after propionate removal. This suggests that Slc4a10 does not play a major role for acid extrusion at the time window analyzed (Fig. 2a, b).

Progressive Auditory Impairment and Reduction of the Endocochlear Potential in Slc4a10 Knockout Mice

Since Slc4a10 is expressed in the inner ear, we assessed whether disruption of Slc4a10 affects hearing. Already starting at 2 weeks of age, the hearing threshold as determined by auditory-evoked brain stem responses (ABR) to click stimuli was increased by roughly 40 dB in Slc4a10 knockout mice in a C57BL/6J background (Fig. 3a). Suggesting a rapid deterioration, hearing loss was almost 80 dB at 6 months of age. In wild-type mice, hearing thresholds slowly increased over time, consistent with the age-dependent hearing loss reported for C57BL/6J wild-type mice (Henry and Chole 1980).

To assess whether the function of the stria vascularis is compromised, we measured the EP, which is highly dependent on metabolism and ion transport. Already at 2 weeks of age, around hearing onset, the EP was decreased to 45.3 ± 7.9 mV in knockout compared with 102.7 ± 6.9 mV in wild-type mice and remained significantly below wild-type levels (Fig. 3b).

Slc4a10 Knockout Mice Lose Outer Hair Cells While Inner Hair Cells Are Preserved

We addressed whether progressive hearing loss is paralleled by morphological changes of the inner ear. The spiral ganglion and the fibrocyte layer appeared intact at 20 (Fig. 4a, b; middle part of the cochlear duct) and 60 weeks of age (Fig. 4e, f). Semithin sections (Fig. 4c, d) and paraffin sections (Fig. 4g, h) of the stria vascularis did not reveal obvious alterations. Because the thickness of the stria vascularis appeared quite variable between different individuals and because of previous reports (Potter et al. 2016), we also quantified its thickness in the middle part of the cochlear duct for 4 WT and 5 KO mice at 60 weeks of age. The thickness was not significantly changed in knockout mice (Fig. 4i). Moreover, the number of nuclei in 8-µm thick sections of the stria vascularis did not differ between

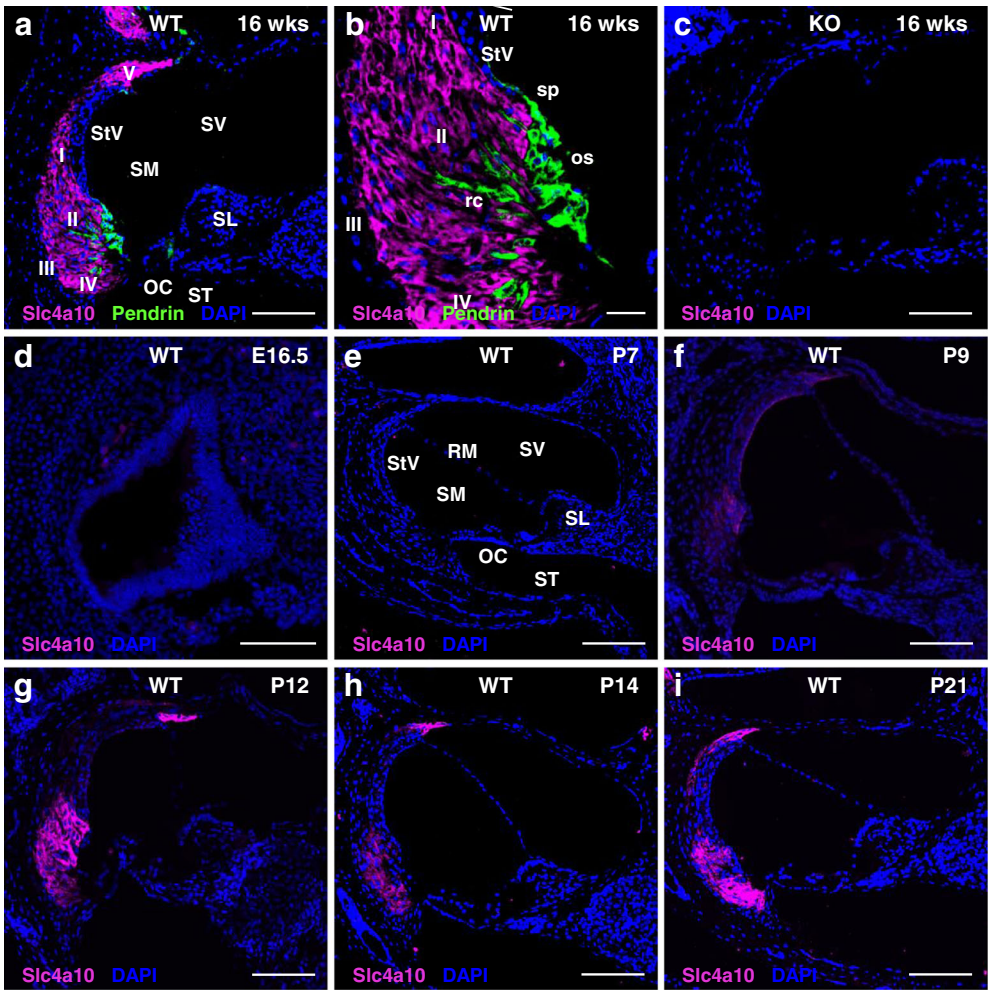

Fig. 1. Slc4a10 expression in spiral ligament fibrocytes starts shortly before hearing onset in mice. **a** Section of the lower part of the cochlear duct of an adult (16-week-old) wild-type mouse stained for Slc4a10 (magenta) and Pendrin (green). Slc4a10 is expressed in the spiral ligament. It is not expressed in the stria vascularis or the organ of Corti. **b** Magnification from (**a**). Slc4a10 expression is restricted to type I, II, IV, and V fibrocytes and does not include root cells, outer sulcus cells, or spiral prominence epithelial cells, which express Pendrin. **c** The specificity of the Slc4a10 antibody was confirmed by the absence of labeling in corresponding Slc4a10 KO sections. **d–i** Expression of Slc4a10 in the developing inner ear. At embryonal day 16.5 (E16.5) (**d**) and postnatal day 7 (P7) (**e**), Slc4a10 is not yet expressed in the inner ear. At P9 (**f**), the Slc410 signal is weak and restricted to type II and V fibrocytes. At P12 (**g**) and P14 (**h**), Slc4a10 is clearly expressed in spiral ligament fibrocyte types II and V. At P21 (**i**), the labeling also includes type I and IV fibrocytes. OC, Organ of Corti; os, outer sulcus epithelial cells; rc, root cells; RM, Reissner's membrane; SL, spiral limbus; SM, scala media; sp, spiral prominence epithelial cells; ST, scala tympani; StV, stria vascularis; SV, scala vestibuli. The fibrocyte subtypes I–V are indicated. Nuclei are visualized by DAPI staining (blue). Scale bars, **a**, **c**, and **e–i** 120 µm; **b** 30 µm; **d** 100 µm

genotypes in the middle part of the cochlear duct (Fig. 4j).

Because of the strong expression of Slc4a10 in fibrocytes of the lateral wall of the cochlea of WT mice, we also quantified fibrocyte nuclei in 8-µm thick sections of the basal, middle, and apical part of the spiral ligament of 4 WT and 5 KO mice at 60 weeks of age. Again, no difference was observed between genotypes (Fig. 4k).

Closer analysis of the organ of Corti in the middle part of the cochlear duct (Fig. 5a, b) revealed a loss of outer hair cells in knockout mice at 20 weeks of age, whereas inner hair cells were preserved. For quantification of outer hair cells, we dissected and stained the organ of Corti from Slc4a10 wild-type and knockout inner ears with phalloidin conjugated to Alexa 555 at different time points to visualize the stereocilia of outer and inner hair cells (Fig. 5c–j). While hair cells were largely preserved up to 3 weeks of age (Fig. 5k, l), there was a progressive loss of outer hair cells at 6 and 24 weeks of age in knockout mice (Fig. 5m, n).

Disruption of Slc4a10 Does Not Affect Gjb2 and Gjb6 Expression in Spiral Ligament Fibrocytes while Slc4a7 Expression Is Lost

The phenotype of Slc4a10 knockout mice closely resembles the phenotypes of inner ear specific Gjb2

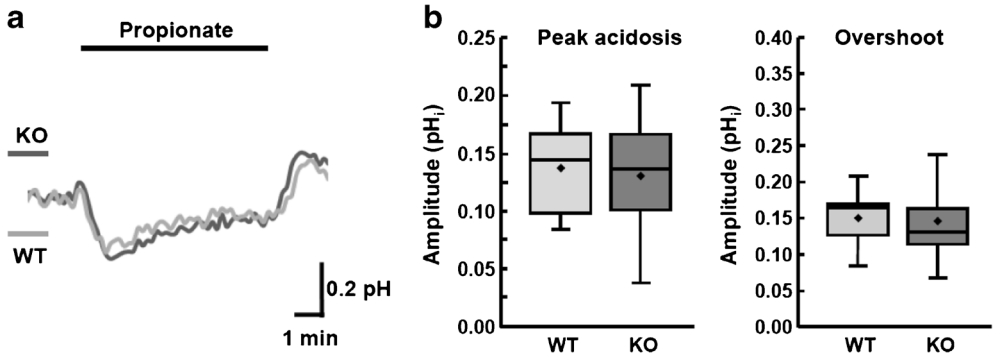

Fig. 2. Acid extrusion is not severely disturbed in explanted spiral ligament fibrocytes of P12 Slc4a10 knockout mice. **a** pH_i recordings from WT and KO spiral ligament fibrocytes (mean from recordings of 24 KO and 15 WT fibrocytes from ≥ 5 mice per genotype). The intracellular acid load was induced by bath application of 20 mM propionate (horizontal bar). Upward deflections indicate an increase in the pH_i. **b** Columns represent the maximal peak acidosis (delta pH_i) induced by propionate and amplitudes of the alkaline overshoot during propionate washout, respectively (mean ± standard error of means). No difference in the maximal peak acidosis in response to propionate (ΔpH WT, 0.137 ± 0.0342; ΔpH KO, 0.131 ± 0.0528; T_{38}, $t = 0.406$, $p = 0.69$, two-sided Student's t test) and the alkaline overshoot after propionate removal (ΔpH WT, 0.149 ± 0.0372; KO, 0.145 ± 0.0652; T_{38}, $t = 0.541$, $p = 0.85$, two-sided Student's t test) suggests that Slc4a10 does not play a major role for acid extrusion at the time window analyzed

and Gjb6 knockout mice (Cohen-Salmon et al. 2002; Teubner et al. 2003). Therefore, we assessed the distribution pattern and protein abundance of Gjb2 and Gjb6 proteins in Slc4a10 knockout mice, which did not differ between genotypes (Fig. 6a, b).

We also assessed whether the disruption of Slc4a10 might have an effect on Slc4a7 expression in spiral ligament fibrocytes. Notably, we detected at least two major bands for Slc4a7 and Slc4a10 in immunoblots of spiral ligament lysates. These bands likely correspond with different splice variants of the respective proteins, as previously reported (Romero et al. 2013). Surprisingly, Slc4a7 could not be detected in spiral ligament lysates of Slc4a10 knockout mice at 3, 6, and 56 weeks of age (Fig. 7a, b), while the expression in other tissues such as the brain, kidney, and pancreas was preserved (Fig. 7b). Immunostainings of cochlea sections confirmed a loss of Slc4a7 immunoreactivity in the spiral ligament of Slc4a10 knockout mice, while Slc4a10 expression was preserved in the spiral ligament of Slc4a7 knockout cochleae (Fig. 7c–f).

Because cell shrinkage and clear spaces in the extracellular matrix between spiral ligament fibrocytes had been reported for 12-week-old Slc4a7 knockout mice (Lopez et al. 2005), we assessed the structure and ultrastructure of fibrocytes for wild-type and Slc4a10 knockout mice more closely. Although we did not observe obvious cell shrinkage or increased

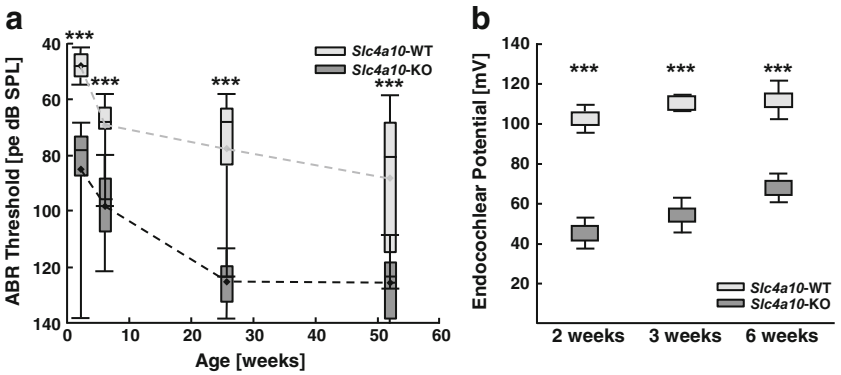

Fig. 3. Early onset auditory impairment and reduction of the endocochlear potential in Slc4a10 knockout mice. **a** Hearing thresholds were determined by auditory brain stem recordings in response to click stimuli. Compared with wild-type littermates (dotted gray line), hearing thresholds of Slc4a10 knockout mice (dotted black line) are significantly decreased at 2, 6, 26, and 52 weeks of age. Repeated-measures two-way ANOVA with Bonferroni post-test, *** $p < 0.0005$. Boxes depict 25th, median, and 75th percentiles and whiskers the 5th/95th percentile range. **b** In knockout mice, the endocochlear potential is decreased to 45.2 ± 7.9 mV compared with 102.7 ± 6.9 mV in wild-type mice (KO $n = 6$, WT $n = 5$) at 2 weeks of age. It remains significantly below wild-type levels at 3 weeks (KO 54.3 ± 8.7 mV vs 110.6 ± 3.3 mV; KO $n = 10$, WT $n = 5$) and 6 weeks of age (KO 68.0 ± 7.1 mV vs 112.2 ± 9.9 mV; KO $n = 4$, WT $n = 3$). Repeated-measures two-way ANOVA with Bonferroni post-test, ***$p < 0.0005$. Vertical bars indicate standard deviations

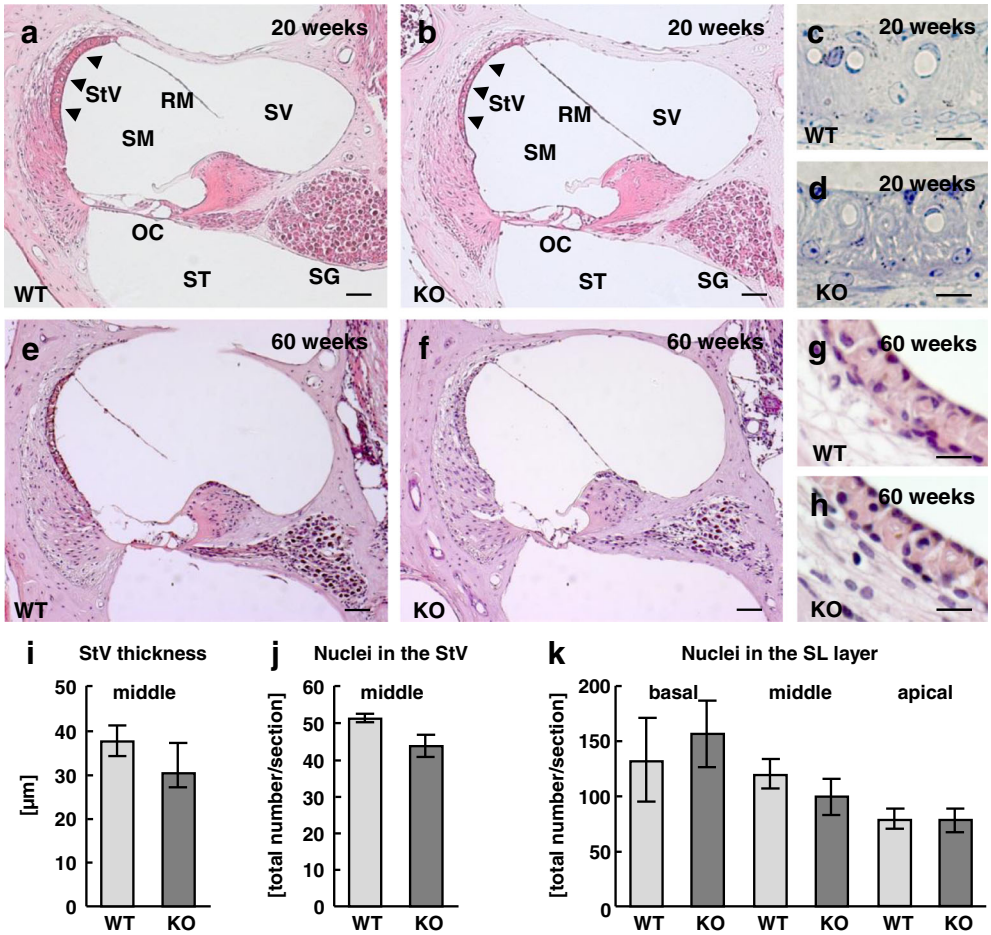

Fig. 4. At early stages, the anatomy of the inner ear of Slc4a10 knockout mice is roughly intact. **a**, **b** As in wild-type (**a**), the gross morphology of HE stained sections of the middle part of the cochlear duct appears intact in 20-week-old Slc4a10 knockout mice (**b**). **c**, **d** Toluidine blue stained semi-thin sections of the stria vascularis from the middle part of the cochlear duct of 20-week-old wild-type and knockout mice. **e**, **f** At 60 weeks of age, the spiral ganglion, the stria vascularis, and the spiral ligament appear intact in the middle part of the cochlear duct of wild-type (**e**) and knockout (**f**) mice. **g**, **h** Higher magnifications of the stria vascularis in the middle part of the cochlear duct of wild-type and knockout mice. **i** Quantification of the thickness of the stria vascularis in 60-week-old WT (37.69 ± 3.52 µm, $n = 4$) and KO (32.15 ± 5.02 µm, $n = 5$) mice. **j** Quantification of the nuclei within the stria vascularis of 60-week-old mice (WT $n = 4$ and KO $n = 5$). **k** Quantification of the nuclei within the spiral ligament of 60-week-old mice (WT $n = 4$ and KO $n = 5$). Scale bars, in **a**, **b**, **e**, and **f** 80 µm; in **c** and **d** 10 µm; **g** and **h** 30 µm. OC, organ of Corti; RM, Reissner's membrane; SG, spiral ganglion; SM, scala media; ST, scala tympani; SV, scala vestibuli

spaces between cells in semi-thin sections (Fig. 8a, d), the ultrastructural analysis revealed alterations of mitochondria in fibrocytes in 14-week-old knockout mice. These alterations were absent in the control mice (Fig. 8b, c, e, f). To get a better idea about the mitochondrial pool in fibrocytes, we stained cochlea sections for the mitochondrial protein cytochrome C (Fig. 8g–k). Overall, the distribution of cytochrome C signals appeared unaltered in 24-week-old Slc4a10 knockout mice compared with wild-type (Fig. 8h–k). This impression was bolstered by the quantification of signal pixels in type II fibrocytes per area (WT 15.51 ± 2.22 % vs KO 13.44 ± 3.62 % (mean ± standard deviation), 3 mice per genotype with 2 sections each, $p = 0.20$, two-sided Student's t test). Notably, we did not detect any co-localization of cytochrome C and Slc4a10, suggesting that Slc4a10 does not localize to mitochondria (Fig. 8g, h).

DISCUSSION

This study confirms that the HCO_3^- transporter Slc4a10 is expressed in inner ear fibrocytes and that its disruption causes hearing loss characterized by a diminished EP and a loss of outer hair cells. In contrast to the study by Potter et al., which reported an increase of the auditory threshold to clicks by roughly 30 dB at 9 months of age (Potter et al. 2016), the phenotype in our Slc4a10 knockout mouse model was already obvious at 2 weeks of age. This striking difference may be explained by a

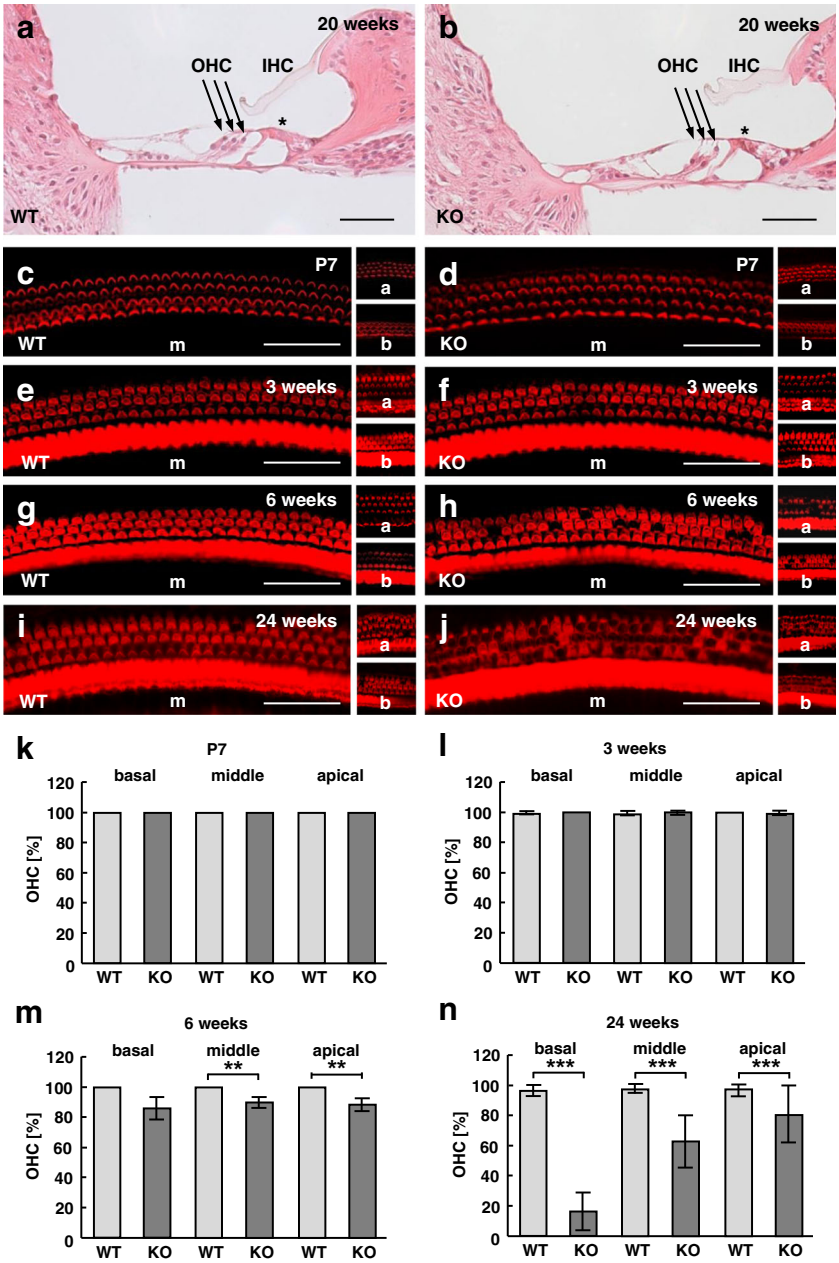

Fig. 5. Outer hair cells are progressively lost in Slc4a10 knockout mice. **a**, **b** Magnifications of the organ of Corti in HE stained sections of the middle part of the cochlear duct at 20 weeks of age show outer hair cell loss. **c–j** Representative images taken from phalloidin stained whole mounts of the basal (b), middle (m), and apical (a) part of the cochlear duct at P7 (**c**, **d**), 3 (**e**, **f**), 6 (**g**, **h**), and 24 weeks of age (**i**, **j**). **k–n** Quantification of outer hair cells in the basal, middle, and apical part of the cochlear duct at the age of P7 (k; $n = 2$ per genotype), 3 (l; $n = 3$ per genotype), 6 (m; $n = 3$ per genotype), and 24 (n; $n = 5$ per genotype) weeks of age (two-sided Student's t test; $^{**}p < 0.005$, $^{***}p < 0.0005$). Scale bars, **a**, **b** 40 µm; **c–j** 35 µm

difference in the genetic background of mice used in the two studies. Instead of the mixed C3H.Pde6bþ+ background (Potter et al. 2016), we used mice which had been backcrossed with C57BL/6J for at least 15 generations. Because congenic breeding theoretically results in a congenic strain with 99.9 % genetic identity to the target strain after 10 generations (Markel et al. 1997), our study was performed in an almost pure C57BL/6J background. Inbred strains of mice vary widely in onset and severity of age-related hearing loss, an important consideration when assessing hearing in mutant mice (Johnson et al. 2006). C57BL/6J mice, in particular, are known to develop age-dependent hearing loss (Henry and Chole 1980). This likely explains, why we observed a late onset hearing loss in our wild-type cohort. It will be interesting to identify the genetic modifier(s) specific to C57BL/6J that are responsible

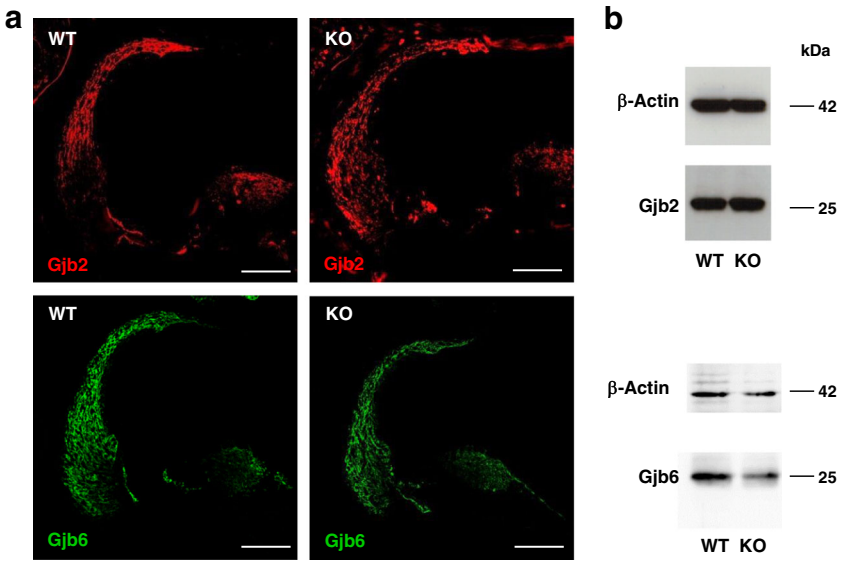

Fig. 6. Gjb2 and Gjb6 expressions are not altered upon disruption of Slc4a10. **a** The distribution of Gjb2 and Gjb6 is not altered in Slc4a10 knockout mice. Scale bars, 100 µm. **b** Immunoblot analysis of lysates from spiral ligaments do not suggest an alteration of Gjb2 or Gjb6 protein abundance in Slc4a10 knockout mice (samples were pooled from $n = 3$ mice for each genotype). Beta-actin served as a loading control

for this aggravation of the inner ear phenotype observed in Slc4a10 knockout mice in the future. It will require additional experiments such as appropriate linkage crosses.

Notably, the EP was already decreased in 2-week-old Slc4a10 knockout mice. The EP is generated in the stria vascularis, where the apical membrane of intermediate cells of the stria vascularis is highly permeable for K^+. This allows effective K^+ uptake at

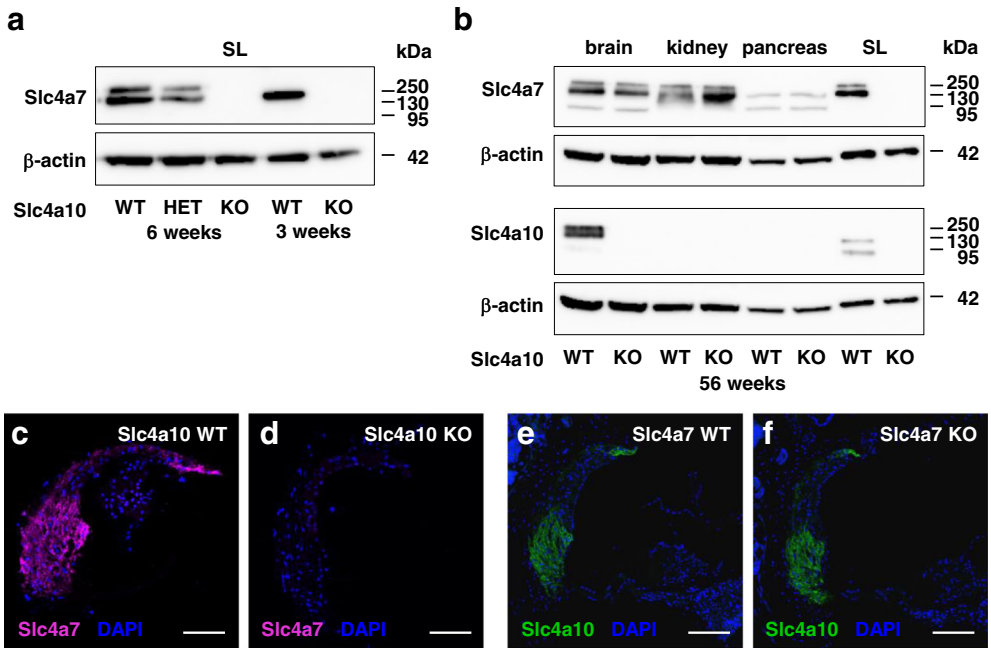

Fig. 7. Expression of Slc4a7 is lost in spiral ligament fibrocytes upon disruption of Slc4a10. **a** Immunoblot analysis shows lack of Slc4a7 expression in protein lysates of spiral ligaments of Slc4a10 knockout mice and decreased Slc4a7 protein abundance in heterozygous (HET) Slc4a10 knockout mice at the age of 3 and 6 weeks of age (samples were pooled from $n = 3$ mice for each genotype and age). **b** Slc4a7 protein abundance in the brain, kidney, or pancreas protein lysates is preserved in 56-week-old Slc4a10 knockout mice but absent in spiral ligament lysates ($n = 3$ per genotype). **c**, **d** The Slc4a7 labeling (magenta) of fibrocytes is lost in Slc4a10 knockout mice ($n = 2$ mice). **e**, **f** The Slc4a10 labeling of spiral ligament fibrocytes (green) is preserved in Slc4a7 knockout mice ($n = 2$ mice). Nuclei are stained with DAPI (blue). Scale bars, **c**–**f** 100 µm

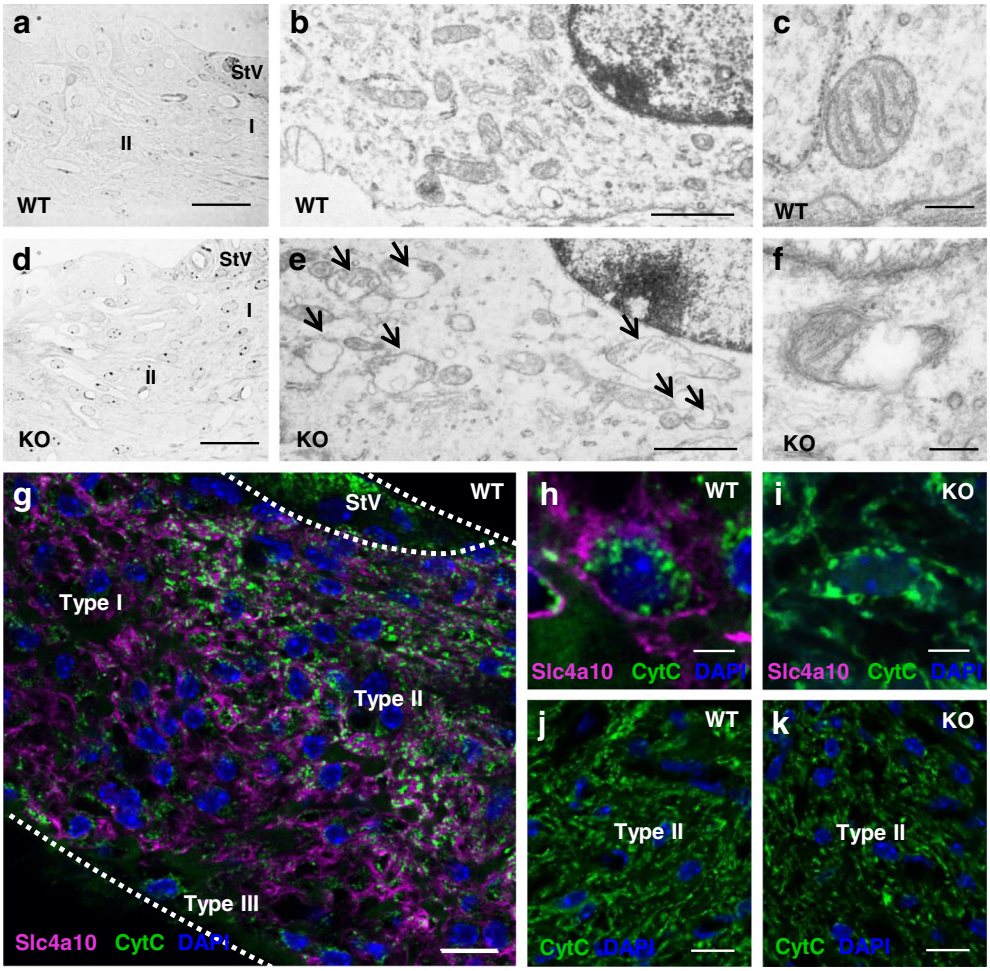

Fig. 8. Mitochondria in fibrocytes of Slc4a10 knockout mice are altered. **a**–**f** Morphological analysis of the spiral ligament. Semi-thin sections from the basal part of the cochlea of a 24-week-old wild-type (**a**) or knockout (**d**) mouse suggest that the regular structure of the spiral ligament is preserved in Slc4a10 knockout mice. The ultrastructural analysis of spiral ligament fibrocytes of 14-week-old controls (**b**, **c**) compared with Slc4a10 knockout mice (**e**, **f**) reveals mitochondrial alterations (arrows) in knockout mice ($n = 3$ mice per genotype). **g**–**i** Co-stainings for Slc4a10 (magenta) and the mitochondrial protein cytochrome C (green) of the spiral ligament. **g** Overview of a stained spiral ligament obtained from a 24-week-old wild-type mouse. A higher magnification (**h**) reveals that Slc4a10 localizes to the fibrocyte plasma membrane, while the cytochrome C signals localize to intracellular structures. The Slc4a10 signal is absent in knockout fibrocytes (**i**). **j**, **k** At 24 weeks of age, cytochrome C signals (green) do not differ between genotypes (wild-type (**j**) and knockout (**k**), $n = 3$ per genotype). Nuclei are stained with DAPI (blue). Scale bars, **a** and **d** 30 µm; **b** and **e** 1 µm; **g** 10 µm; in **c** and **f** 0.2 µm; **h** and **i** 5 µm; **j** and **k** 15 µm. StV, stria vascularis

the basolateral site of marginal cells via the NaK2Cl cotransporter NKCC1, which is then secreted apically into the endolymph. Because the EP increases the driving force for K^+ influx into hair cells and thus their sensitivity, this can explain the increase in the auditory threshold even before outer hair cells are lost. Although the thickness of the stria vascularis appeared quite variable, the quantification of its thickness and its cell number did not differ between genotypes. This suggests that the stria vascularis remained structurally intact upon disruption of Slc4a10 in a C57BL/6J background. This is in contrast to previous findings in the C3H.Pde6b background (Potter et al. 2016).

Intermediate cells, basal cells, pericytes, endothelial cells, and fibrocytes of the spiral ligament are joined by gap junctions that may facilitate movements of K^+ and/or metabolites towards the endolymph. Most gap junctions in this network are formed by heteromeric complexes of GJB2 (Cx26) and GJB6 (Cx30) (Petit 2006). Consistent with an essential role for hearing, mutations of GJB2 (Cx26) and GJB6 (Cx30) are the most prevalent causes of hereditary childhood deafness (Parker and Bitner-Glindzicz 2015). Fibrocytes of the spiral ligament also express GJB3 (Cx31) and GJB1 (Cx32) (Lopez-Bigas et al. 2002), which are also associated with deafness (Lang et al. 2007). Since the coupling of fibrocytes appears to be an essential prerequisite for inner ear function,

we addressed whether Gjb2 or Gjb6 expression levels are altered upon disruption of Slc4a10. Overall protein abundance of both gap junction proteins as assessed by Western blot or immunofluorescence studies was unchanged. Nevertheless, the phenotype of Slc4a10 knockout mice closely resembles that of mice with a targeted disruption of Gjb6 (Teubner et al. 2003) or of mice with an epithelial cell specific disruption of Gjb2. These are characterized by a decrease of the EP and a progressive loss of outer hair cells while leaving inner hair cells intact (Cohen-Salmon et al. 2002).

Since Slc4a10 mediates HCO_3^- transport and the conductance of gap junctions is influenced by intracellular pH (Spray et al. 1981; Francis et al. 1999; Stergiopoulos et al. 1999; Palacios-Prado et al. 2010), we hypothesized that loss of Slc4a10 might impair the coupling of fibrocytes by gap junctions via its effect on intracellular pH. However, the pH regulation of acutely dissected spiral ligaments from P11 to P13 mice was not changed, and the peak acidosis in response to propionic acid and the ensuing recovery did not differ between genotypes. Potentially, the time window for our analysis may have been too early to detect subtle differences in pH regulation, since Slc4a10 expression further increases after hearing onset. Unfortunately, the dissection of the spiral ligament at a later time point was hampered by the progressive ossification of the bony capsule of the inner ear. Moreover, cultured primary fibrocytes rapidly lost Slc4a10 expression (data not shown).

Still, a functional impairment of inner ear fibrocyte pH regulation is an attractive hypothesis. Indeed, disruption of two other acid extruders expressed in inner ear fibrocytes, i.e., Slc4a7 and Slc4a11, also causes hearing loss. This expression in the inner ear resembles that of Slc4a10 (Bok et al. 2003; Groger et al. 2010). Like Slc4a10 knockout mice, Slc4a11 knockout mice also show only minor anatomical changes and a reduction of the EP. The phenotype of Slc4a7 knockout mice seems to be more severe, because they progressively lose outer and inner hair cells, type II and IV fibrocytes, supporting cells, and spiral ganglion neurons beginning around P30 (Bok et al. 2003; Lopez et al. 2005). Compared with Slc4a10, Slc4a7 expression in the inner ear appears broader and may also include the organ of Corti, inner, and outer sulcus cells (Lopez et al. 2005). Notably, its expression in fibrocytes was lost upon disruption of Slc4a10, while its expression was preserved in other tissues. Our histological analysis of Slc4a10 knockout mice does not support a massive loss of fibrocytes up to 60 weeks of age. Again, differences in the genetic background may contribute to these discrepancies. At the ultrastructural level, however, we found mitochondrial alterations in spiral ligament fibrocytes of Slc4a10 knockout mice. Mitochondrial damage is a characteristic finding in several mouse models of age-related hearing loss and is often attributed to increased oxidative stress (Le Calvez et al. 1998; Mahendrasingam et al. 2011; Han and Someya 2013). To solve the mechanistic link between Slc4a10 and Slc4a7 expression will be an interesting but challenging question for the future.

This study shows that Slc4a10 expression in the inner ear coincides with the establishment of the EP during postnatal day 7 and 14 (Sadanaga and Morimitsu 1995) and is exclusively restricted to type I, II, IV, and V fibrocytes that also express Slc4a7. Surprisingly, both Slc4a10 and Slc4a7 expression is lost in inner ear fibrocytes of Slc4a10 knockout mice. In a C57Bl/6J background, this causes an early onset decrease of the EP and hearing loss. Our data link inner ear phenotypes of Slc4a10 and Slc4a7 knockout mice and demonstrate the importance of the genetic background when studying auditory function in mice.

ACKNOWLEDGEMENTS

We thank Cynthia Halvorson for the final editing of the manuscript.

AUTHOR CONTRIBUTIONS

H.M, A.M., S.N., T.H.: performed experiments, analyzed data, and wrote the paper.

A.K..: performed experiments, analyzed data, and wrote the paper.

J.P.: provided material and wrote the paper.

C.A.H.: initiated the study, supervised experiments, and wrote the paper.*Funding* This study was funded by grants of the DFG to C.A.H. (HU 800/5-1 and HU 800/8-1).

COMPLIANCE WITH ETHICAL STANDARDS

All experiments were approved by the responsible local institution (Landesamt für Lebensmittelsicherheit und Verbraucherschutz, Bad Langensalza and Niedersächsisches Landesamt für Verbraucherschutz und Lebensmittelsicherheit, Germany) and comply with the ARRIVE guidelines.

Competing Interests The authors declare that they have no conflict of interest.

Publisher's Note Springer Nature remains neutral with regard to jurisdictional claims in published maps and institutional affiliations.

REFERENCES

BOEDTKJER E, PRAETORIUS J, MATCHKOV VV, STANKEVICIUS E, MOGENSEN S, FUCHTBAUER AC, SIMONSEN U, FUCHTBAUER EM, AALKJAER C (2011) Disruption of Na^+,HCO_3^- cotransporter NBCn1 (slc4a7) inhibits NO-mediated vasorelaxation, smooth muscle Ca^{2+} sensitivity, and hypertension development in mice. Circulation 124:1819–1829

BOETTGER T, HUBNER CA, MAIER H, RUST MB, BECK FX, JENTSCH TJ (2002) Deafness and renal tubular acidosis in mice lacking the K-Cl co-transporter Kcc4. Nature 416:874–878

BOETTGER T, RUST MB, MAIER H, SEIDENBECHER T, SCHWEIZER M, KEATING DJ, FAULHABER J, EHMKE H, PFEFFER C, SCHEEL O, LEMCKE B, HORST J, LEUWER R, PAPE HC, VOLKL H, HUBNER CA, JENTSCH TJ (2003) Loss of K-Cl co-transporter KCC3 causes deafness, neurodegeneration and reduced seizure threshold. EMBO J 22:5422–5434

BOK D, GALBRAITH G, LOPEZ I, WOODRUFF M, NUSINOWITZ S, BELTRANDELRIO H, HUANG W, ZHAO S, GESKE R, MONTGOMERY C, VAN SLIGTENHORST I, FRIDDLE C, PLATT K, SPARKS MJ, PUSHKIN A, ABULADZE N, ISHIYAMA A, DUKKIPATI R, LIU W, KURTZ I (2003) Blindness and auditory impairment caused by loss of the sodium bicarbonate cotransporter NBC3. Nat Genet 34:313–319

COHEN-SALMON M, OTT T, MICHEL V, HARDELIN JP, PERFETTINI I, EYBALIN M, WU T, MARCUS DC, WANGEMANN P, WILLECKE K, PETIT C (2002) Targeted ablation of connexin26 in the inner ear epithelial gap junction network causes hearing impairment and cell death. Curr Biol 12:1106–1111

DESIR J, MOYA G, REISH O, VAN REGEMORTER N, DECONINCK H, DAVID KL, MEIRE FM, ABRAMOWICZ MJ (2007) Borate transporter SLC4A11 mutations cause both Harboyan syndrome and non-syndromic corneal endothelial dystrophy. J Med Genet 44:322–326

EVERETT LA, BELYANTSEVA IA, NOBEN-TRAUTH K, CANTOS R, CHEN A, THAKKAR SI, HOOGSTRATEN-MILLER SL, KACHAR B, WU DK, GREEN ED (2001) Targeted disruption of mouse Pds provides insight about the inner-ear defects encountered in Pendred syndrome. Hum Mol Genet 10:153–161

FRANCIS D, STERGIOPOULOS K, EK-VITORIN JF, CAO FL, TAFFET SM, DELMAR M (1999) Connexin diversity and gap junction regulation by pHi. Dev Genet 24:123–136

GROGER N, FROHLICH H, MAIER H, OLBRICH A, KOSTIN S, BRAUN T, BOETTGER T (2010) SLC4A11 prevents osmotic imbalance leading to corneal endothelial dystrophy, deafness, and polyuria. J Biol Chem 285:14467–14474

HAN C, SOMEYA S (2013) Mouse models of age-related mitochondrial neurosensory hearing loss. Mol Cell Neurosci 55:95–100

HENNINGS JC, PICARD N, HUEBNER AK, STAUBER T, MAIER H, BROWN D, JENTSCH TJ, VARGAS-POUSSOU R, ELADARI D, HUBNER CA (2012) A mouse model for distal renal tubular acidosis reveals a previously unrecognized role of the V-ATPase a4 subunit in the proximal tubule. EMBO mol med 4:1057–1071

HENRY KR, CHOLE RA (1980) Genotypic differences in behavioral, physiological and anatomical expressions of age-related hearing loss in the laboratory mouse. Audiology 19:369–383

HILGEN G, HUEBNER AK, TANIMOTO N, SOTHILINGAM V, SEIDE C, GARRIDO MG, SCHMIDT KF, SEELIGER MW, LOWEL S, WEILER R, HUBNER CA, DEDEK K (2012) Lack of the sodium-driven chloride bicarbonate exchanger NCBE impairs visual function in the mouse retina. PLoS One 7:e46155

JACOBS S, RUUSUVUORI E, SIPILA ST, HAAPANEN A, DAMKIER HH, KURTH I, HENTSCHKE M, SCHWEIZER M, RUDHARD Y, LAATIKAINEN LM, TYYNELA J, PRAETORIUS J, VOIPIO J, HUBNER CA (2008) Mice with targeted Slc4a10 gene disruption have small brain ventricles and show reduced neuronal excitability. Proc Natl Acad Sci U S A 105:311–316

JOHNSON KR, ZHENG QY, NOBEN-TRAUTH K (2006) Strain background effects and genetic modifiers of hearing in mice. Brain Res 1091:79–88

LANG F, VALLON V, KNIPPER M, WANGEMANN P (2007) Functional significance of channels and transporters expressed in the inner ear and kidney. Am J Physiol 293:C1187–C1208

LE CALVEZ S, AVAN P, GILAIN L, ROMAND R (1998) CD1 hearing-impaired mice. I: distortion product otoacoustic emission levels, cochlear function and morphology. Hear Res 120:37–50

LOPEZ IA, ACUNA D, GALBRAITH G, BOK D, ISHIYAMA A, LIU W, KURTZ I (2005) Time course of auditory impairment in mice lacking the electroneutral sodium bicarbonate cotransporter NBC3 (slc4a7). Brain Res 160:63–77

LOPEZ-BIGAS N, ARBONES ML, ESTIVILL X, SIMONNEAU L (2002) Expression profiles of the connexin genes, Gjb1 and Gjb3, in the developing mouse cochlea. Mech Dev 119(Suppl 1):S111–S115

MAHENDRASINGAM S, MACDONALD JA, FURNESS DN (2011) Relative time course of degeneration of different cochlear structures in the CD/1 mouse model of accelerated aging. JARO 12:437–453

MARKEL P, SHU P, EBELING C, CARLSON GA, NAGLE DL, SMUTKO JS, MOORE KJ (1997) Theoretical and empirical issues for marker-assisted breeding of congenic mouse strains. Nat Genet 17:280–284

PALACIOS-PRADO N, BRIGGS SW, SKEBERDIS VA, PRANEVICIUS M, BENNETT MV, BUKAUSKAS FF (2010) pH-dependent modulation of voltage gating in connexin45 homotypic and connexin45/connexin43 heterotypic gap junctions. Proc Natl Acad Sci U S A 107:9897–9902

PARK M, LI Q, SHCHEYNIKOV N, ZENG W, MUALLEM S (2004) NaBC1 is a ubiquitous electrogenic Na^+-coupled borate transporter essential for cellular boron homeostasis and cell growth and proliferation. Mol Cell 16:331–341

PARKER M, BITNER-GLINDZICZ M (2015) Genetic investigations in childhood deafness. Arch Dis Child 100:271–278

PARKER MD, MUSA-AZIZ R, ROJAS JD, CHOI I, DALY CM, BORON WF (2008) Characterization of human SLC4A10 as an electroneutral Na/HCO3 cotransporter (NBCn2) with Cl^- self-exchange activity. J Biol Chem 283:12777–12788

PETIT C (2006) From deafness genes to hearing mechanisms: harmony and counterpoint. Trends Mol Med 12:57–64

PETIT C, LEVILLIERS J, HARDELIN JP (2001) Molecular genetics of hearing loss. Annu Rev Genet 35:589–646

POTTER PK, BOWL MR, JEYARAJAN P, WISBY L, BLEASE A, GOLDSWORTHY ME, SIMON MM, GREENAWAY S, MICHEL V, BARNARD A, AGUILAR C, AGNEW T, BANKS G, BLAKE A, CHESSUM L, DORNING J, FALCONE S, GOOSEY L, HARRIS S, HAYNES A, HEISE I, HILLIER R, HOUGH T, HOSLIN A, HUTCHISON M, KING R, KUMAR S, LAD HV, LAW G, MACLAREN RE, MORSE S, NICOL T, PARKER A, PICKFORD K, SETHI S, STARBUCK B, STELMA F, CHEESEMAN M, CROSS SH, FOSTER RG, JACKSON IJ, PEIRSON SN, THAKKER RV, VINCENT T, SCUDAMORE C, WELLS S, EL-AMRAOUI A, PETIT C, ACEVEDO-AROZENA A, NOLAN PM, COX R, MALLON AM, BROWN SDM (2016) Novel gene function revealed by mouse mutagenesis screens for models of age-related disease. Nat Commun 7:12444

ROMERO MF, CHEN AP, PARKER MD, BORON WF (2013) The SLC4 family of bicarbonate (HCO_3^-) transporters. Mol Asp Med 34:159–182

SADANAGA M, MORIMITSU T (1995) Development of endocochlear potential and its negative component in mouse cochlea. Hear Res 89:155–161

SINNING A, LIEBMANN L, HUBNER CA (2015) Disruption of Slc4a10 augments neuronal excitability and modulates synaptic short-term plasticity. Front Cell Neurosci 9:223

SPICER SS, SCHULTE BA (1991) Differentiation of inner ear fibrocytes according to their ion transport related activity. Hear Res 56:53–64

SPRAY DC, HARRIS AL, BENNETT MV (1981) Gap junctional conductance is a simple and sensitive function of intracellular pH. Science 211:712–715

STERGIOPOULOS K, ALVARADO JL, MASTROIANNI M, EK-VITORIN JF, TAFFET SM, DELMAR M (1999) Hetero-domain interactions as a mechanism for the regulation of connexin channels. Circ Res 84:1144–1155

TEUBNER B, MICHEL V, PESCH J, LAUTERMANN J, COHEN-SALMON M, SOHL G, JAHNKE K, WINTERHAGER E, HERBERHOLD C, HARDELIN JP, PETIT C, WILLECKE K (2003) Connexin30 (Gjb6)-deficiency causes severe hearing impairment and lack of endocochlear potential. Hum Mol Genet 12:13–21

WANG CZ, YANO H, NAGASHIMA K, SEINO S (2000) The Na^+-driven Cl^-/HCO_3^- exchanger. Cloning, tissue distribution, and functional characterization. J Biol Chem 275:35486–35490

WANGEMANN P, ITZA EM, ALBRECHT B, WU T, JABBA SV, MAGANTI RJ, LEE JH, EVERETT LA, WALL SM, ROYAUX IE, GREEN ED, MARCUS DC (2004) Loss of KCNJ10 protein expression abolishes endocochlear potential and causes deafness in Pendred syndrome mouse model. BMC Med 2:30